Hand-sized dielectric barrier discharge reactor of floating potential electrode for cell model studies

L. Asimakoulas[1], M. Katsafadou[1], P. Svarnas[1], K. Pachis[2], N. Kostazos[2], K. Gazeli[1], E. Mitronikas[3], S. G. Antimisiaris[2,4]

[1]*University of Patras, Department of Electrical and Computer Engineering, High Voltage Laboratory, 26 504 Rion-Patras, Greece*
[2]*University of Patras, Department of Pharmacy, Pharmaceutical Technology Laboratory, 26 504 Rion-Patras, Greece*
[3]*University of Patras, Department of Electrical and Computer Engineering, Electromechanical Conversion Lab., 26 504 Rion-Patras, Greece*
[4]*Institute of Chemical Engineering Sciences FORTH/ICE-HT, 26 504 Rion-Patras, Greece*

A miniaturized dielectric barrier discharge reactor of floating potential electrode is designed and fabricated mainly for biomedical applications. The reactor is hand-sized and electrically shielded for adaptive and safe use, respectively. The system is driven by sinusoidal high voltage at audio frequencies, and it is here characterized with electrical and optical emission analyzes. The efficiency of the reactor for parametric studies of bio-systems is proven by means of membrane studies on cell models (liposomes).

1. Introduction

Atmospheric pressure discharges producing plasmas out of thermodynamic equilibrium have been applied to biomedical field widely. Sterilization, skin regeneration, tooth bleaching, cancer cell necrosis, are just a few examples [1].

Towards this direction, our group has recently initiated studies on the influence of atmospheric pressure plasmas on membrane models [2,3], as a suitable method to explore fundamental mechanisms of plasma-induced effects on cells. Following our first report [2], increasing interest has been noticed. Different cell-mimics and biochemical reporters have been used for testing the role of various plasma species on membrane disruption and RONS delivery [4-6]. In most cases, plasma setups with a continuous flow of noble gas are used for such studies.

Another approach with high practical interest is the Floating Electrode Dielectric Barrier Discharge (FE-DBD) [7]. In this configuration, the discharge is sustained between the dielectric barrier of the driven electrode and the specimen surface being of free (floating) potential. An obvious advantage in this case is the use of the ambient air as operating gas. Although FE-DBD reactors have already given very promising results in biomedicine [7-15], their functionality on membrane models has not yet been demonstrated. The main claim of the present work refers to this task by testing a hand-sized portable DBD reactor operating in a FE-like mode for liposomal membrane disruption.

2. Experimental setup and Liposome Specimens

2.1. Reactor and power supply

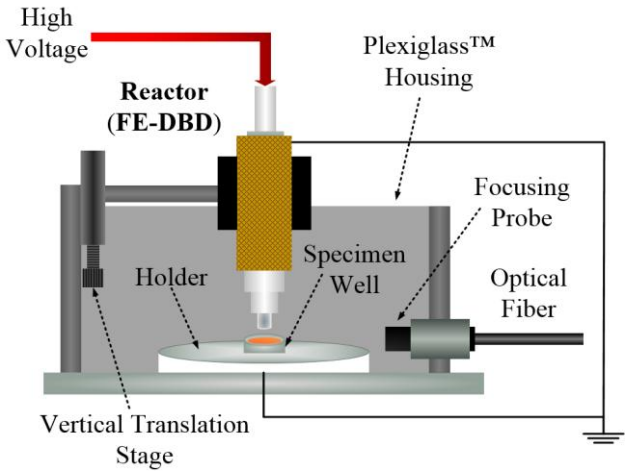

Fig. 1. Schematic diagram of the FE-DBD reactor installed in protective housing for liposome treatment. The holder and the specimen well are both grounded.

The conceptual view of the setup during liposome treatment is shown in **Fig. 1**. The main part consists of the reactor which appears coaxial geometry and has a total length of about 135 mm. The single electrode is a stainless steel rod (8 mm in diam.) covered with 2 mm in thickness quartz which acts as the discharge dielectric barrier. The external body of the reactor is made from brass and it is 36 mm in (external) diameter. This shield is grounded directly for protection against electric shock and it has

embossed textured finish for stable handling. The electric power is fed through a high voltage bushing installed on the top. The reactor has been successfully tested for continuous operation at ambient air on the timescale of hours with voltages up to 25 kV peak-to-peak / 10 kHz. The power supply is a home-made one delivering 10 kHz sinusoidal waveforms with amplitude up to 30 kV peak-to-peak and maximum current 50 mA rms. The total harmonic distortion on resistive load is less than 1%.

Finally, the reactor is mounted on a vertical translation stage for micro-adjustment of the discharge gap and enclosed in a Plexiglas™ housing opened on the top. This limits the disturbance of the specimen as much as possible while at the same time the discharge takes place at ambient conditions. The bottom of the housing is an aluminium optical breadboard where the holder of the specimen well is fixed and grounded. The specimen well is made from stainless steel (inner diam. 21 mm and depth 7 mm). It has a flat bottom and its inner surface is well polished. Tests on control specimens (liposomes and cells) have shown none effect on them due to the contact with the metallic surface.

2.2. Electrical and optical measurements

The applied voltage $u(t)$ is monitored through a high voltage divider (Tektronix P6015, DC – 75 MHz). The circuit current $i(t)$ is recorded with a wideband current transformer (Pearson Electronics 6585, 40 Hz – 250 MHz) clamped around the high voltage cable. Both signals are recorded on a digital oscilloscope (LeCroy WaveRunner 44Xi-A, 400 MHz–5 GSamples/s). The discharge mean power $\bar{P}$ is estimated over ten successive voltage cycles T as (**Fig. 2**)

$$\bar{P} = \frac{1}{10T}\int_{-5T}^{5T} u(t)i(t)dt \qquad (1)$$

Simultaneously, light emitted from the entire discharge gap is collected with a one-lens probe (Newport 77646, UV-visible) used here for focusing parallel light rays. For this purpose, the lens is placed at a distance of several times its effective focal length (19 mm) from the discharge axis (**Fig. 1**) and a liquid light guide (Newport 77556, UV-visible) is fixed on its focal point. The light detector is a Hamamatsu Ltd electron photo-multiplier tube (PMT, R928, 185–900 nm) terminated at one of the 50 Ω inputs of the above oscilloscope.

Alternatively, the liquid light guide is replaced by an optical fiber (Ceramoptec UV 1500/1590N) connected to a high resolution monochromator (Jobin Yvon, THR 1000, 170–750 nm, 2400 grooves/mm) for optical emission spectroscopy (OES) measurements. The optical assembly is calibrated in terms of wavelength units and relative spectral efficiency with the Newport 6035 and 6333 lamps, respectively. Finally, the rotational temperature of probe molecules is estimated by fitting theoretical to experimental rotational distributions [16].

2.3 Liposome preparation and treatment

Two types of liposomes (LIPs) are subjected to treatment, i.e. small uni-lamellar (SUV) and large multi-lamellar (MLV) vesicles. They contain egg L-a-phosphatidylcholine (PC) and pure cholesterol (Chol), and they are prepared under strict protocol described previously [2,3]. The ratio PC/Chol 1:1 (mol/mol) is used here for both LIPs-types.

A small hydrophilic fluorescent dye, calcein, is entrapped in the interior aqueous compartment of the liposomes in a quenched concentration. Its release from the vesicles is measured before and immediately after the subjection to plasma treatment, as a measure of vesicle integrity. Briefly, 10 μl are drawn out from each incubation tube and diluted with 4 ml of 10 mM phosphate buffer saline (pH 7.40). 0.5 ml of this dilution is then further diluted with 3.5 ml buffer for avoiding fluorescence intensity saturation. The fluorescence intensity of the specimen is then measured before and after the addition of surfactant Triton X-100 at a final concentration of 1% v/v. The measurements are performed with a Shimadzu RF-1501 fluorescence spectrophotometer (emission 470 nm, excitation 520 nm), thermostated at 37±1°C through a Julabo FS18 refrigerated and heated circulator. The percentage of calcein retained (%Retention) in the LIPs is determined from the %Latency equation, i.e.

$$\%Latency = \left[1 - \frac{1}{1.1}\left(\frac{F_{BT}}{F_{AT}}\right)\right] x\ 100 \qquad (2)$$

where F_{BT} and F_{AT} stands for the calcein fluorescence intensity before and after the addition of Triton X-100, respectively (F_{AT} is corrected appropriately for sample dilution). Following treatment, %Retention is calculated as the percentage of the before-plasma latency of each liposome formulation.

3. Results and Discussion

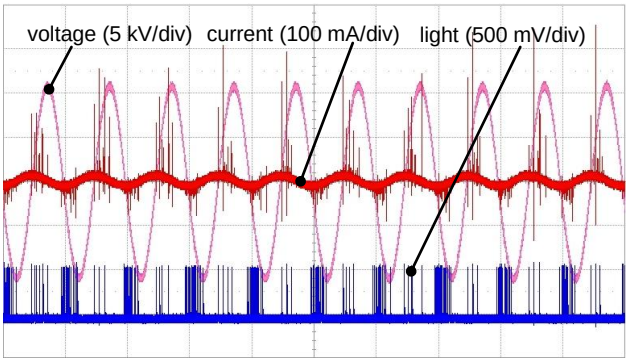

Fig. 2. Typical voltage, current and light waveforms over ten periods of the applied voltage (1 mm discharge gap, 23 kV peak-to-peak, 100 μs/div, without specimen).

The PMT signal is in good correlation with the current impulses, showing the impulsive emission of the discharge due to its filamentary form. Interestingly, numerous light impulses appear during the negative slope of the applied voltage, as they are compared with the light impulses during the positive slope. This intense emission could be attributed to excitations induced by the acceleration of the electrons that have previously accumulated on the surface of the dielectric during the positive half cycle of the voltage and which are now subjected to negative potential (negative half cycle) [17].

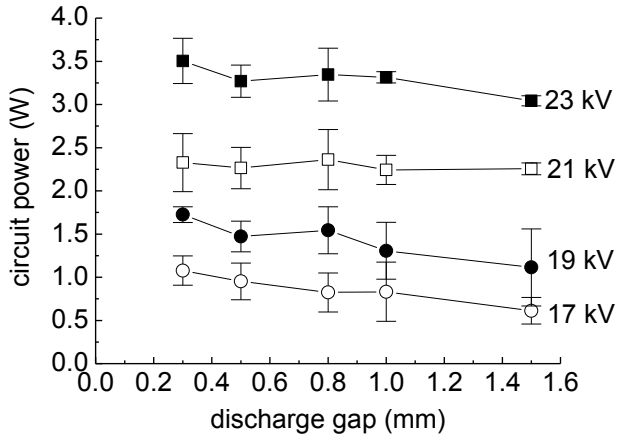

Fig. 3. Mean power (see Eq. 1) delivered to the system (without specimen) as a function of the discharge gap, with the applied voltage (peak-to-peak) as parameter. Mean values and standard deviations from three experimental series are given.

Fig. 3 depicts the mean operation power of the reactor versus the inter-electrode gap for various amplitudes of the driving high voltage. The low power consumption is underlined and it is mainly affected by the voltage than the gap.

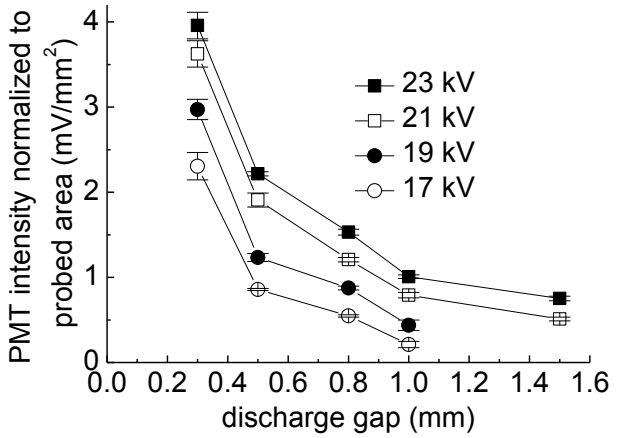

Fig. 4. Normalized mean values of the optical emission intensity integrated over time (PMT) and space (entire discharge gap), as a function of the gap distance, with the applied voltage (peak-to-peak) as parameter. Mean values and standard deviations from three experimental series are given.

Fig. 4 illustrates the strong dependence of the optical emission intensity on the discharge gap and the driving voltage. The mean values of the PMT output signals are normalized to the surface defined by the gap dimensions. A simple rectangular geometry is assumed (electrode diameter x gap distance). This is necessary since the probed emissive area changes with the gap.

Since the discharge emission is related to emissive reactive species production (like ROS and RNS), **Figs. 3**, **4** are of great importance for adjusting the treatment conditions for intended applications.

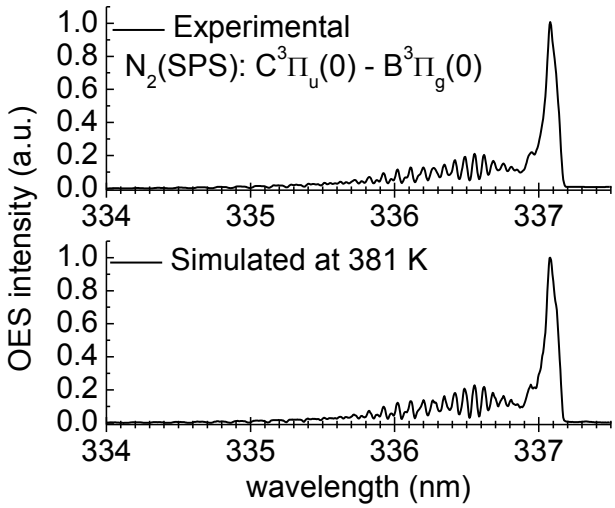

Fig. 5. Typical experimental and simulated optical emission spectra (resolution 0.005 nm) of the rotational distribution of the N_2(SPS) band corresponding to the transition $C^3\Pi_u(0) - B^3\Pi_g(0)$ (1 mm discharge gap, 23 kV peak-to-peak, without specimen). For 17-23 kV peak-to-peak the gas temperature does not change significantly.

The wide scan OES pattern of the discharge (not shown here) showed mainly excited N_2(SPS) and N_2^+(FNS), while OH and NOγ with much weaker OES intensity were also detected. The rotational distribution of the band corresponding to the head/transition $C^3\Pi_u(0) - B^3\Pi_g(0)$ is selected (**Fig. 5**) and a gas temperature close to 381 K (~108 ^oC) is calculated. Similar values are obtained from other bands of the N_2(SPS). The actual temperature in the aqueous solution is certainly lower.

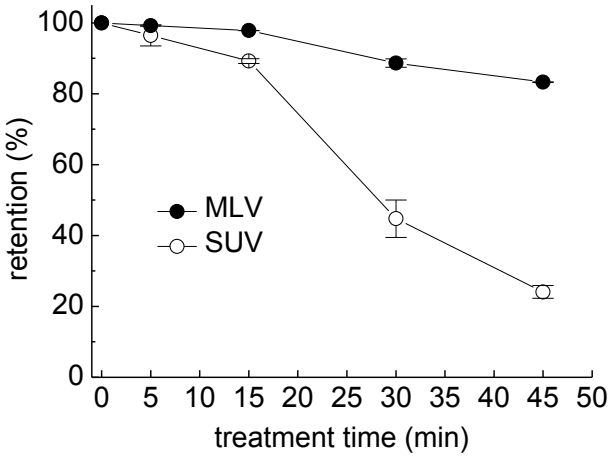

Fig. 6. Effect of the FE-DBD reactor on SUV and MLV liposomes treated for various times (19 kV peak-to-peak, ~1 mm gap between the dielectric and aqueous solution surfaces). Mean values and standard deviations from two experimental series are given.

In **Fig. 6** the results from the application of the above characterized reactor on SUV and MLV liposome treatment are summarized. It is clear that the reactive species produced (or other synergetic factors) are able to disrupt the liposomal membranes extensively (see [2,3] for possible mechanisms). MLV liposomes are more rigid due to the numerous membranes surrounding their hydrophilic core, rather than a single membrane (SUV case).

4. Conclusions

In this introductory work, dielectric barrier discharge of floating electrode was proposed as a very efficient medium to disturb membranes of liposomes. The reactor presented can thus been used for fundamental studies on cells by experimentally modelling the cells with liposomes of different features (e.g. size, composition etc). The consumed mean power was less than 5 W and different reactive species were produced. The gas temperature in the bulk discharge was found to be ~108 ^oC, but the temperature in the aqueous solution was lower.

5. References

[1] Th. von Woedtke, S. Reuter, K. Masura, K.-D. Weltmann, Phys. Rep. **530** (2013) 291–320

[2] P. Svarnas, S. H. Matrali, K. Gazeli, Sp. Aleiferis, F. Clement,S. G. Antimisiaris, Appl. Phys. Lett. **101** (2012) 264103

[3] P. Svarnas, S. H. Matrali, K. Gazeli, S. G. Antimisiaris, "*Assessment of atmospheric-pressure guided streamer (plasma bullet) influence on liposomes with different composition and physicochemical properties*", Plasma Process. Polym. (2015) submitted

[4] S.-H. Hong, E. J. Szili, A. Toby A. Jenkins, R. D. Short, J. Phys. D: Appl. Phys. **47** (2014) 362001

[5] R. Tero, Y. Suda, R. Kato, H. Tanoue, H. Takikawa, Appl. Phys. Express **7** (2014) 077001

[6] M.U. Hammer, E. Forbrig, S. Kupsch, K.-D. Weltmann, S. Reuter, Plasma Medicine **3(1–2)** (2013) 97–114

[7] G. Fridman, M. Peddinghaus, H. Ayan. A. Fridman, M. Balasubramanian, A. Gutsol, A. Brooks, G. Friedman, Plasma Chem. Plasma Process. **26** (2006) 425–442

[8] G. Fridman, A. Shereshevsky, M. M. Jost, A. D. Brooks, A. Fridman, A. Gutsol, V. Vasilets, G. Friedman, **27** (2007) 163-176

[9] M. Cooper, G. Fridman, A. Fridman, S. G. Joshi, J. Appl. Microbiol. **109** (2010) 2039–2048

[10] D. Dobrynin, K. Wasko, G. Friedman, A. Fridman, G. Fridman, Plasma Medicine, **1(2)** (2011) 109–114

[11] D. Dobrynin, G. Fridman, G. Friedman, A. Fridman, Plasma Medicine **2(1-3)** (2012) 71–83

[12] S. Emmert, F. Brehmer, H. Hänßle, A. Helmke, N. Mertens, R. Ahmed, D. Simon, D. Wandke, M. P. Schön, W. M.-Friedrichs, W. Viöl, G. Däschlein, Plasma Medicine, **2(1-3)** (2012) 19–32

[13] E. Curran, R. Duffy, D. Peretz, S. Park, B. Seiber, R. Smalley, A. Raghavan, M. Gurjar, D. Dobrynin, K. Wasko, A. Fridman, G. Fridman, D. Pao, Plasma Medicine **3(3)** (2013) 153-172

[14] S. Kalghatgi, C. Kelly, E. Cerchar, J. A.-Clifford, Plasma Medicine **1(3–4)** (2011) 249–263

[15] N. Y. Babaeva, M. J. Kushner, J. Phys. D: Appl. Phys. **43** (2010) 185206

[16] R. P. Cardoso, T. Belmonte, P. Keravec, F. Kosior, G. Henrion, J. Phys. D: Appl. Phys. **40** (2007) 1394–1400

[17] M. Laroussi, X. Lu, V. Kolobov, R. Arslanbekov, J. Appl. Phys. **96(5)** (2004) 3028–3030